POLYACRYLONITRILE-BASED COMPOSITE CARBON NANOFIBERS WITH TAILORED MICROPOROSITY

E.S. Vtyurina	ves1809@yandex.ru
Ig.I. Ponomarev	gagapon@ineos.ac.ru
A.G. Buyanovskaya	analyst@ineos.ac.ru
I.I. Ponomarev	ivan.ponomarev84@gmail.com
K.M. Skupov	kskupov@ineos.ac.ru

**A.N. Nesmeyanov Institute of Organoelement Compounds
of Russian Academy of Sciences, Moscow, Russian Federation**

Abstract

Carbon nanofibers are currently used in many applications including electrochemical power sources, particularly, fuel cells. Their properties are highly dependent on the micro- and mesoporous structure. Here we provide a porosimetric analysis of the polyacrylonitrile-based electrospun composite Zr- and Ni-containing carbon nanofiber mats by N_2 and CO_2 adsorption methods for the first time. It was found that pyrolysis temperature affects specific surface area and volume: the values increase for the sample pyrolyzed at 900 °C compared with the initial stabilized nanofibers (300 °C, air) according to the Dubinin — Radushkevich, non-local density functional theory (NLDFT) and grand canonical Monte-Carlo methods (GCMC). For higher pyrolysis temperatures (1000 and 1200 °C), the porosimetric parameters decrease compared with the one pyrolyzed at 900 °C. According to the NLDFT and GCMC pore size distribution, the difference for pyrolyzed samples is mostly related to a sharp decrease in the specific surface area for pores with a size of ~ 0.5 nm and an increase for pores at 0.55–0.8 nm compared with the initial stabilized sample. The study demonstrates a way to adjust porosimetric parameters depending on the pyrolysis conditions of the nanofiber mats, since it can improve characteristics of such type of carbon materials in electrochemical devices

Introduction. The shape and geometry of pores as well as their specific volume, specific surface area and pore size distribution are extremely important for the materials used in the electrochemical power sources. In general, the porous structure may play an even more important role than the electrocatalyst activity since it is strongly related to the mass transfer optimization [1–4]. The hydrogen-air high-temperature polymer electrolyte membrane (HT-PEM) fuel cells are a very important type of fuel cell because it allows operation with hydrogen contaminated with CO at 150–200 °C [5, 6]. HT-PEM fuel cell on polybenzimidazole/o-phosphoric acid (PBI/H_3PO_4) membrane usually operates with electrodes with platinum nanoparticle electrocatalyst dispersed on carbon black due to its high specific surface area and relevant porous structure. However, carbon black is unstable under long-term high temperature (150–200 °C) acidic operating conditions. So that, for further HT-PEM fuel cell development, its replacement with more stable carbon nanostructured materials, for example, carbon nanofibers (CNF), is required [7–23].

Materials capable of high CO_2 uptake are becoming important due to the need to develop CO_2 capture and transfer technologies to prevent the climate change. Some activated carbons are known for the mentioned purpose [24]. Nevertheless, finding ways to tailor the CNF porous structure and, consequently, their properties is highly important.

Earlier [25–35] we have shown the possibility of an HT-PEM fuel cell operation with polyacrylonitrile (PAN) or polyheteroarylene based electrospun pyrolyzed CNF electrodes and PBI-OPhT membrane developed in our laboratory. Addition of small amounts (~ 5 wt. % relative to PAN) of carbon black (Vulcan® or Ketjenblack®) into PAN electrospinning solution significantly increased the uniformity of the material, improved the electrospinning process and increased the mechanical strength of pyrolyzed mats, but had almost no effect on the specific surface area of the material. The replacement of such types of carbon black with cheaper and more affordable in terms of import substitution technical carbon (carbon black) UM-76 (UM) is of great importance.

It has been established [36, 37] that optimization of the porous structure, in particular, reducing the excessive microporosity, positively affects the performance of the fuel cell (FC). The obtained results indicate the emerging need to find ways of tuning of the porosimetric characteristics such as specific surface area and volume of the pores and their pore size distribution.

In the given study, the CO_2 adsorption method (at 273 K) was applied to the novel Zr and Ni nanoparticle containing PAN-UM composite pyrolyzed carbon nanofiber mats in order to calculate porosimetric characteristics according

to the Dubinin — Radushkevich, non-local density functional theory and grand canonical Monte-Carlo methods for the first time.

Data and methods for solving problems, accepted assumptions. The composite polymer nanofibers were obtained by the string electrospinning [38–40] method (where multiple jets are generated from the string under high voltage) from an electrospinning polymer solution which contained 3.25 g of PAN with $M_w = 150 \cdot 10^3$ Da, 0.1 g of UM-76 (~3 wt. % relative to PAN), 0.03 g of zirconium (IV) chloride and 0.37 g of nickel (II) acetate well dispersed in 50 mL of DMF during 3 h in ultrasonic bath. The electrospinning was carried out on NS Lab Nanospider™ setup (Elmarco, Czech Republic) at relative humidity of 8 % with the distance between electrodes of 190 mm at the voltage of 69 kV.

The obtained polymer nanofiber mat was stabilized (oxidized) at 300 °C in air (2 h) to make the material suitable for pyrolysis (**1**) [41]. In order to obtain CNF [42, 43], on the next step, the material was pyrolyzed under vacuum ($2 \cdot 10^{-5}$ mbar) at 900, 1000 and 1200 °C (CNF mats **2**, **3** and **4** respectively).

The elemental composition was determined using a CHN analyzer equipped with a Vario Micro Cube thermal desorption column (Elementar, Germany). Zirconium and nickel were determined by the X-ray fluorescence analysis using a VRA-30 X-ray fluorescence spectrometer (Carl Zeiss, Germany).

The in-plane electrical conductivity of the pyrolyzed mats was measured with a RLC E7-8 setup (Belarus) equipped with a four-point probe. The sample thickness was determined using an eXacto ElektroPhysik thickness gage (Germany) and comprised 51 ± 5 μm.

Scanning electron microscopy (SEM) images were obtained with a Hitachi TM4000 SEM tabletop microscope in the back-scattered electron mode at 15 kV of accelerating voltage.

Nitrogen and carbon dioxide adsorption isotherms of the samples were obtained at 77 and 273 K respectively using a 3P Micro 200 Surface Area and Pore Size Analyzer (3P Instruments GmbH and Co. KG, Germany). The Brunauer — Emmett — Teller (BET) equation was applied to nitrogen adsorption isotherms according to the Rouquerol criteria [44]. For microporosity studies, the Dubinin — Radushkevich (DR), non-local density functional theory (NLDFT) [44] and grand canonical Monte-Carlo (GCMC) [44] methods were applied to carbon dioxide adsorption isotherms using NovaWin (version 11.04), Quantachrome Instruments, considering CO_2 cross-sectional area A of 0.21 nm², adsorbed CO_2 density $\rho_{ads} = 1.044$ g $\cdot$ mL^{-1} and $p_0 = 3.485$ MPa, the affinity coefficient β was taken as 0.35 [45]. CO_2 uptake was calculated at standard temperature and pressure (according to IUPAC) of 273 K and 1 bar [46].

Results. After pyrolysis, the shape of the CNF mats was saved. Also, it was found that the materials possess a nanofiber structure (Fig. 1), as confirmed by scanning electron microscopy.
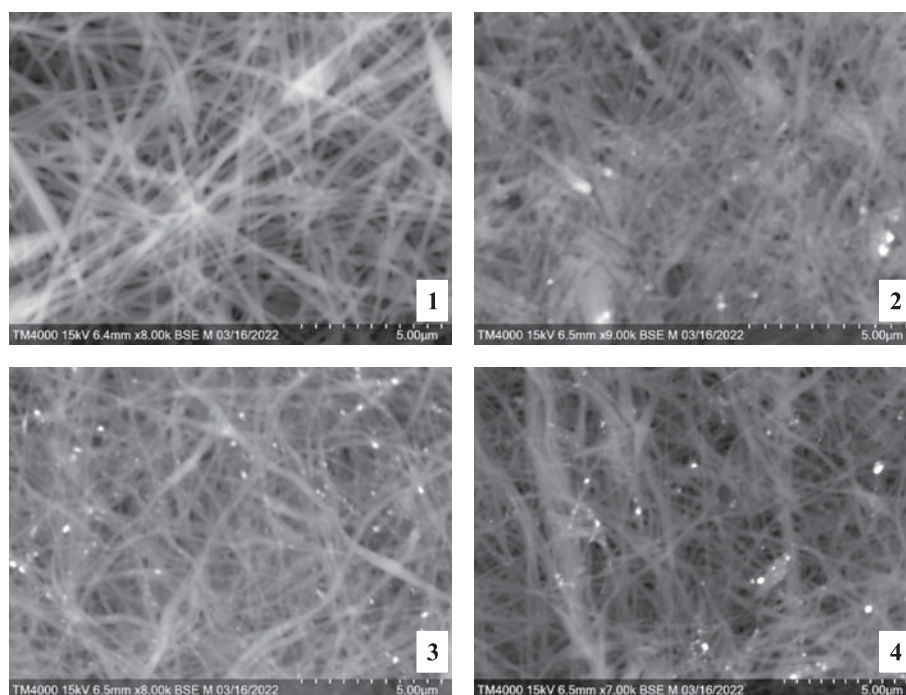

Fig. 1. SEM images of **1** (300 °C, air, 1 atm), **2** (300 °C, air, 1 atm; 900 °C, vacuum, $2 \cdot 10^{-5}$ mbar), **3** (300 °C, air, 1 atm; 1000 °C, vacuum, $2 \cdot 10^{-5}$ mbar) and **4** (300 °C, air, 1 atm; 1200 °C, vacuum, $2 \cdot 10^{-5}$ mbar)

More precise observation of the SEM images of the samples reveals slightly lower nanofiber diameters for the pyrolyzed samples **2**–**4** 50–300 nm compared with 80–400 nm for the initial stabilized sample **1**. However, precise determination of the nanofiber diameters is difficult due to not very high resolution of the SEM setup. Elemental analysis and electrical conductivity data for the samples are shown in Table 1.

Table 1

In-plane electrical conductivity σ of the nanofiber mats measured by a four-point probe and their elemental analysis, %

Sample	σ, S · cm^{-1}	C	N	H	Zr	Ni
1	–	54.7	18.2	2.6	0.6	3.7
2	14.2	83.9	3.8	0.6	0.5	7.9
3	16.2	86.6	2.3	0.6	0.6	6.6
4	29.3	82.0	0.7	0.3	0.5	6.8

As can be seen from Table 1, an increase in the pyrolysis temperature from 900 to 1200 °C leads to a decrease in the nitrogen content from 3.8 to 0.7 wt. % and an increase in the electrical conductivity from 14.2 to 29.3 $S \cdot cm^{-1}$ which could be explained by higher degree of graphitization at higher temperature. Attempts to determine the specific surface area and total pore volume by low-temperature N_2 adsorption (77 K) method using the BET equation were unsuccessful due to the inaccessibility of micropores for N_2 molecules at such a low temperature. As a result, the measurable specific surface area was only 5–15 $m^2 \cdot g^{-1}$. Anyways, the result indicates the limited applicability of the N_2 adsorption method for such type of CNF. The CO_2 adsorption method avoids the kinetic limitations of the adsorbate penetration into micropores, since it is carried out at a higher temperature of 273 K. The micropore specific surface area and specific volume were calculated from the CO_2 adsorption isotherm curves according to the DR, NLDFT and GCMC methods. The isotherm curves and DR plots as well as specific surface area S_{sp} and specific volume V_{sp} data are shown in Fig. 2 and Table 2.
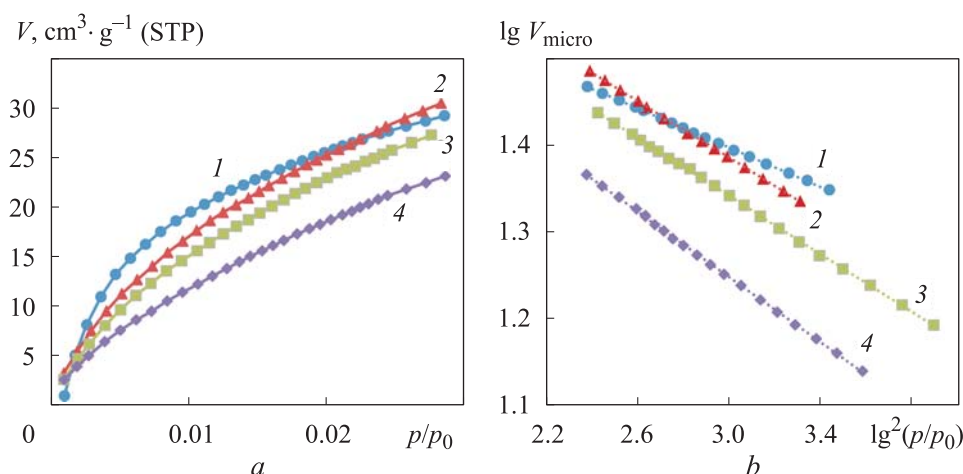

Fig. 2. CO_2 adsorption isotherms (*a*) and DR plots (*b*) for **1** at 300 °C, air, 1 atm (•),
2 at 300 °C, air, 1 atm; 900 °C, vacuum, $2 \cdot 10^{-5}$ mbar (▲), **3** at 300 °C, air, 1 atm;
1000 °C, vacuum, $2 \cdot 10^{-5}$ mbar (■), **4** at 300 °C, air, 1 atm; 1200 °C,
vacuum, $2 \cdot 10^{-5}$ mbar (♦)

Different values of for S_{sp} and V_{sp} obtained by different methods for the same samples are expected since they are related to different physical and mathematical approaches applied in these methods. Slightly higher values for S_{sp} and V_{sp} obtained by the DR method are expectable since the NLDFT and GCMC data are limited by the size of micropores of 1.5 nm, however, the trends

of changes for all the values depending on temperature are the same for all three methods. CO_2 uptake was calculated at standard temperature and pressure (STP) defined as 273 K and 100 kPa according to IUPAC [46].

Table 2

Specific surface area and specific volume by the DR, DFT and GCMC methods and CO₂ uptake data for samples 1–4

Sample	DR		NLDFT		GCMC		CO₂ uptake, mmol/g (1 bar, 273 K)
	S_{sp}, $m^2 \cdot g^{-1}$	V_{sp}, $cm^3 \cdot g^{-1}$	S_{sp}, $m^2 \cdot g^{-1}$	V_{sp}, $cm^3 \cdot g^{-1}$	S_{sp}, $m^2 \cdot g^{-1}$	V_{sp}, $cm^3 \cdot g^{-1}$	
1	308	0.103	305	0.090	282	0.086	1.31
2	424	0.141	312	0.098	340	0.126	1.35
3	392	0.131	291	0.095	276	0.094	1.21
4	367	0.122	243	0.082	252	0.093	1.04

An important difference between the samples, in addition to their specific surface area and volume, is their pore size distribution. Considering the CO_2 adsorption method, the NLDFT and GCMC methods are among the most common for obtaining a pore size distribution. The NLDFT and GCMC pore size distributions are shown on Fig. 3 as the specific surface area derivative dS/dD dependence on the pore diameter D.

Discussion of the results obtained. As can be seen from Table 2, the specific surface area and specific volume of micropores increase after pyrolysis of the initial polymer nanofiber mat at 900 °C (from 308 to 424 $m^2 \cdot g^{-1}$ and from 0.103 to 0.141 $cm^3 \cdot g^{-1}$ respectively) according to the DR method. Similar changes are observed by the NLDFT and GCMC methods. It is accompanied by an increase in carbon content from 54.7 to 83.9 % (see Table 1) and a decrease in nitrogen content from 18.2 to 3.8 % according to the elemental analysis. It reflects the processes of carbonization and graphitization occurring during the pyrolysis of PAN. As a result, the sample becomes electrically conductive and the in-plane electrical conductivity of the mat reaches 14.2 $S \cdot cm^{-1}$ which makes it suitable for use in electrochemical power sources, particularly, as electrodes in fuel cell. An increase of the pyrolysis temperature to 1000 °C leads to a further increase of the electrical conductivity to 16.2 $S \cdot cm^{-1}$ and a further decrease of nitrogen content (2.3 %). At the same time, the specific volume of micropores decreases to 0.131 $cm^3 \cdot g^{-1}$ according to the DR method and also decreases according to the NLDFT and GCMC methods. For the pyrolysis temperature of 1200 °C, the electrical conductivity drastically increases to 29.3 $S \cdot cm^{-1}$,
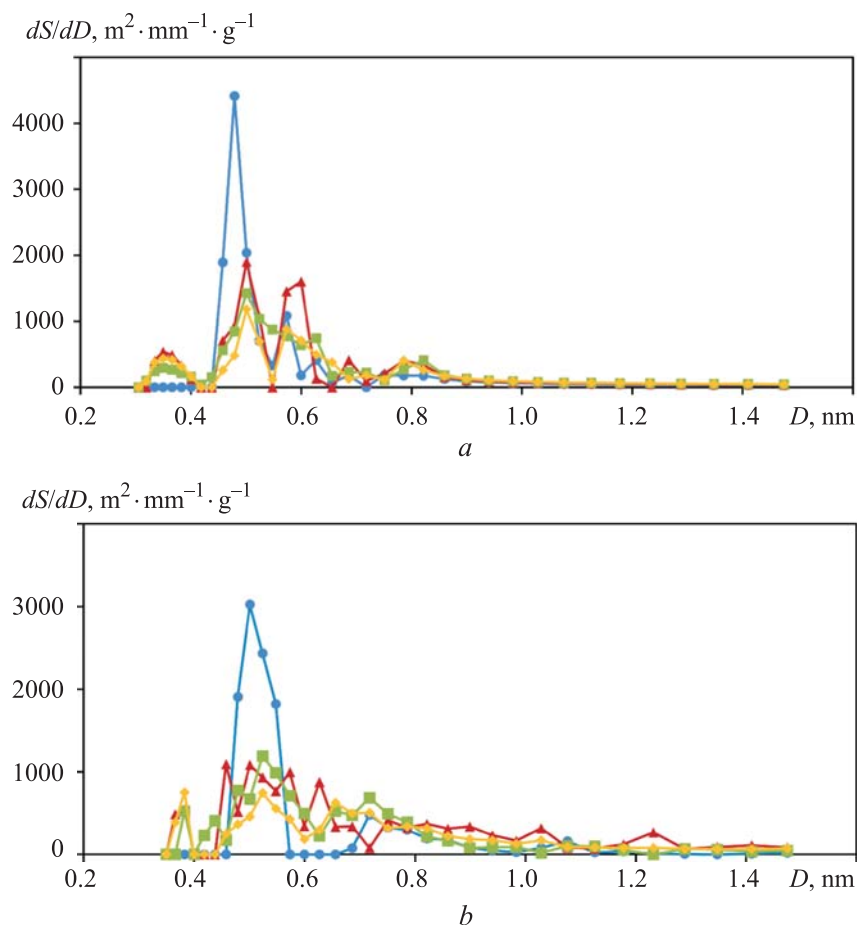
Fig. 3. NLDFT (*a*) and GCMC (*b*) pore size distribution for **1** at 300 °C, air, 1 atm (•),
2 at 300 °C, air, 1 atm; 900 °C, vacuum, $2 \cdot 10^{-5}$ mbar (▲), **3** at 300 °C, air, 1 atm;
1000 °C, vacuum, $2 \cdot 10^{-5}$ mbar (■), **4** at 300 °C, air, 1 atm; 1200 °C,
vacuum, $2 \cdot 10^{-5}$ mbar (♦)

and nitrogen content drops to 0.7 %. The specific surface area and specific volume of micropores continue to decrease. Carbon dioxide uptake follows almost the same trends. It increases slightly when the sample was pyrolyzed at 900 °C (**2**) compared with the initial stabilized sample (**1**) from 1.31 to 1.35 mmol $\cdot$ g^{-1}. Further increase of the pyrolysis temperature (1000 and 1200 °C) leads to lower CO_2 uptake values (1.21 and 1.04 mmol $\cdot$ g^{-1} respectively). The S_{sp} and V_{sp} values for **3** and **4** are closer to the ones of the initial sample **1** according to the DR method or even lower according to the NLDFT and GCMC methods. However, it is unlikely that the pore structure after pyrolysis at 1000 and 1200 °C returns to the one of the original stabilized sample. To verify this point, the pore size distributions were obtained using the

NLDFT and GCMC methods (see Fig. 3). As can be seen from Fig. 3, the NLDFT and GCMC pore size distributions are quite similar, and most of the specific surface area of the samples belong to ultramicropores (< 0.7 nm). After pyrolysis, the specific surface area of pores with a size of ~ 0.5 nm drastically decreases compared with the initial stabilized CNF. However, the specific surface area related with pores less than 0.45 nm and more than 0.55 nm increases, it explains the observed increase in the total micropore surface area for the sample pyrolyzed at 900 °C (**2**) compared with the initial stabilized CNF sample (**1**). At higher pyrolysis temperatures (1000 and 1200 °C), the specific surface area decreases in almost the entire range of micropore sizes compared with the sample pyrolyzed at 900 °C. It explains the observed decrease in the total specific surface area of micropores compared with **2**, which becomes closer to the specific surface area of the initial stabilized CNF (**1**). However, as can be seen from the pore size distributions, the pore structure for pyrolyzed samples is different compared with the one of the initial stabilized CNF (**1**).

Summary. Microporosity of the carbonized materials for electrochemical applications (including electrospun CNF) is extremely important for their practical use. Generally known that such critical issues as phosphoric acid distribution, platinum electrocatalyst deposition, triple point optimization, gas (hydrogen, oxygen or air) diffusion, etc. strongly affect HT-PEM fuel cell performance. Obviously, it is also highly important for electrospun CNF mats when Pt/CNF are used as gas diffusion electrodes (GDE). Here, for the first time, we apply the Dubinin — Radushkevich, NLDFT and GCMC methods to CO_2 adsorption isotherms of PAN-based composite Zr- and Ni-containing electrospun CNF mats to study their microporosity. It was shown that pyrolysis (carbonization) of the polyacrylonitrile composite nanofibers makes them electrically conductive; and, depending on pyrolysis temperature, microporosity can be tuned accordingly. The obtained porosimetric, elemental analysis, microscopy and electrical conductivity data may help to tailor the porosimetric parameters and pore size distribution in order to make CNF mats more suitable for use in different electrochemical power source applications, particularly, as GDEs in the HT-PEM fuel cells. Further development of these materials will allow to improve performance of the HT-PEM fuel cells and will help to produce new materials with high carbon dioxide uptake.

E.S. Vtyurina, Ig.I. Ponomarev, A.G. Buyanovskaya

REFERENCES

[1] Yang L., Shui J., Du L., et al. Carbon-based metal-free ORR electrocatalysts for fuel cells: past, present, and future. *Adv. Mater.*, 2019, vol. 31, iss. 13, art. 1804799. DOI: https://doi.org/10.1002/adma.201804799

[2] Nie Y., Wei Z. Electronic and physical property manipulations: recent achievements towards heterogeneous carbon-based catalysts for oxygen reduction reaction. *Chem-CatChem*, 2019, vol. 11, iss. 24, pp. 5885–5897.
DOI: https://doi.org/10.1002/cctc.201901584

[3] Volfkovich Yu.M., Sosenkin V.E., Bagotsky V.S. Structural and wetting properties of fuel cell components. *J. Power Sources*, 2010, vol. 195, iss. 17, pp. 5429–5441.
DOI: https://doi.org/10.1016/j.jpowsour.2010.03.002

[4] Volfkovich Yu.M., Filippov A.N., Bagotsky V.S. Structural properties of porous materials and powders used in different fields of science and technology. Engineering Materials and Processes. London, New York, Springer, 2014.
DOI: https://doi.org/10.1007/978-1-4471-6377-0

[5] Li Q., Aili D., Hjuler H.A. (eds), et al. High temperature polymer electrolyte membrane fuel cells. Cham, Springer, 2016. DOI: https://doi.org/10.1007/978-3-319-17082-4

[6] Zeis R. Materials and characterization techniques for high-temperature polymer electrolyte membrane fuel cells. *Beilstein J. Nanotechnol.*, 2015, vol. 6, pp. 68–83.
DOI: https://doi.org/10.3762/bjnano.6.8

[7] Araya S.S., Zhou F., Liso V., et al. A comprehensive review of PBI-based high temperature PEM fuel cells. *Int. J. Hydrogen Energ.*, 2016, vol. 41, iss. 46, pp. 21310–21344.
DOI: https://doi.org/10.1016/j.ijhydene.2016.09.024

[8] Zhang J. PEM fuel cell electrocatalysts and catalyst layers. Springer, 2008.

[9] Chandan A., Hattenberger M., El-Kharouf A., et al. High temperature (HT) polymer electrolyte membrane fuel cells (PEMFC) — a review. *J. Power Sources*, 2013, vol. 231, pp. 264–278. DOI: https://doi.org/10.1016/j.jpowsour.2012.11.126

[10] Rosli R.E., Sulong A.B., Daud W.R.W. et al. A review of high-temperature proton exchange membrane fuel cell (HT-PEMFC) system. *Int. J. Hydrogen Energ.,* 2017, vol. 42, iss. 14, pp. 9293–9314. DOI: https://doi.org/10.1016/j.ijhydene.2016.06.211

[11] Myles T., Bonville L., Maric R. Catalyst, membrane, free electrolyte challenges, and pathways to resolutions in high temperature polymer electrolyte membrane fuel cells. *Catalysts,* 2017, vol. 7, iss. 1, art. 16. DOI: https://doi.org/10.3390/catal7010016

[12] Quartarone E., Angioni S., Mustarelli P. Polymer and composite membranes for proton-conducting, high-temperature fuel cells: a critical review. *Materials,* 2017, vol. 10, iss. 7, art. 687. DOI: https://doi.org/10.3390/ma10070687

[13] Delikaya O., Bevilacqua N., Eifert L., et al. Porous electrospun carbon nanofibers network as an integrated electrode-gas diffusion layer for high temperature polymer electrolyte membrane fuel cells. *Electrochim. Acta.,* 2020, vol. 345, art. 136192.
DOI: https://doi.org/10.1016/j.electacta.2020.136192

[14] Borup R., Meyers J., Pivovar B., et al. Scientific aspects of polymer electrolyte fuel cell durability and degradation. *Chem. Rev.*, 2007, vol. 107, no. 10, pp. 3904–3951. DOI: https://doi.org/10.1021/cr050182l

[15] Debe M.K. Electrocatalyst approaches and challenges for automotive fuel cells. *Nature*, 2012, vol. 486, pp. 43–51. DOI: https://doi.org/10.1038/nature11115

[16] Steele B.C.H., Heinzel A. Materials for fuel-cell technologies. *Nature*, 2001, vol. 414, pp. 345–352. DOI: https://doi.org/10.1038/35104620

[17] Arsalis A. A comprehensive review of fuel cell-based micro-combined-heat-and-power systems. *Renew. Sust. Energ. Rev.*, 2019, vol. 105, pp. 391–414.
DOI: https://doi.org/10.1016/j.rser.2019.02.013

[18] Wang Y., Chen K.S., Mishler J., et al. A review of polymer electrolyte membrane fuel cells: Technology, applications, and needs on fundamental research. *Appl. Energ.*, 2011, vol. 88, iss. 4, pp. 981–1007. DOI: https://doi.org/10.1016/j.apenergy.2010.09.030

[19] Myles T., Bonville L., Maric R. Catalyst, membrane, free electrolyte challenges, and pathways to resolutions in high temperature polymer electrolyte membrane fuel cells. *Catalysts*, 2017, vol. 7, iss. 1, art. 16. DOI: https://doi.org/10.3390/catal7010016

[20] Zamora H., Plaza J., Canizares P., et al. Improved electrodes for high temperature proton exchange membrane fuel cells using carbon nanospheres. *ChemSusChem*, 2016, vol. 9, iss. 10, pp. 1187–1193. DOI: https://doi.org/10.1002/cssc.201600050

[21] Jeon Y., Park J.-I., Ok J., et al. Enhancement of catalytic durability through nitrogen-doping treatment on the CNF-derivatized ACF support for high temperature PEMFC. *Int. J. Hydrogen Energy*, 2016, vol. 41, iss. 16, pp. 6864–6876.
DOI: https://doi.org/10.1016/j.ijhydene.2016.03.021

[22] Wang X.X., Tan Z.H., Zeng M., et al. Carbon nanocages: a new support material for Pt catalyst with remarkably high durability. *Sci. Rep.*, 2014, vol. 4, art. 4437.
DOI: https://doi.org/10.1038/srep04437

[23] Chan S., Jankovic J., Susac D., et al. Electrospun carbon nanofiber catalyst layers for polymer electrolyte membrane fuel cells: fabrication and optimization. *J. Mater. Sci.*, 2018, vol. 53, no. 16, pp. 11633–11647. DOI: https://doi.org/10.1007/s10853-018-2411-4

[24] Sharma A., Jindal J., Mittal A., et al. Carbon materials as CO_2 adsorbents: a review. *Environ. Chem. Lett.*, 2021, vol. 19, no. 2, pp. 875–910.
DOI: https://doi.org/10.1007/s10311-020-01153-z

[25] Ponomarev I.I., Zhigalina O.M., Skupov K.M., et al. Preparation and thermal treatmentinfluence on Pt-decorated electrospun carbon nanofiber electrocatalysts. *RSC Adv.*, 2019, vol. 9, iss. 47, pp. 27406–27418. DOI: https://doi.org/10.1039/C9RA05910E

[26] Ponomarev I.I., Skupov K.M., Naumkin A.V., et al. Probing of complex carbon nanofiber paper as gas-diffusion electrode for high temperature polymer electrolyte membrane fuel cell. *RSC Adv.*, 2019, vol. 9, iss. 1, pp. 257–267.
DOI: https://doi.org/10.1039/C8RA07177B

[27] Zhigalina V.G., Zhigalina O.M., Ponomarev I.I., et al. Electron microscopy study of new composite materials based on electrospun carbon nanofibers. *CrystEngComm*, 2017, vol. 19, iss. 27, pp. 3792–3800. DOI: https://doi.org/10.1039/C7CE00599G

[28] Skupov K.M., Ponomarev I.I., Razorenov D.Yu., et al. Carbon nanofiber paper cathode modification for higher performance of phosphoric acid fuel cells on polybenzimidazole membrane. *Russ. J. Electrochem.*, 2017, vol. 53, no. 7, pp. 728–733.
DOI: https://doi.org/10.1134/S1023193517070114

[29] Skupov K.M., Ponomarev I.I., Razorenov D.Y., et al. Carbon nanofiber paper electrodes based on heterocyclic polymers for high temperature polymer electrolyte membrane fuel cell. *Macromol. Symp.*, 2017, vol. 375, no. 1, art. 1600188.
DOI: https://doi.org/10.1002/masy.201600188

[30] Ponomarev I.I., Skupov K.M., Razorenov D.Yu., et al. Electrospun nanofiber pyropolymer electrodes for fuel cells on polybenzimidazole membranes. *Russ. J. Electrochem.*, 2016, vol. 52, no. 8, pp. 735–739.
DOI: https://doi.org/10.1134/S1023193516080097

[31] Ponomarev I.I., Skupov K.M., Ponomarev Iv.I., et al. New gas-diffusion electrode based on heterocyclic microporous polymer PIM-1 for high-temperature polymer electrolyte membrane fuel cell. *Russ. J. Electrochem.*, 2019, vol. 55, no. 6, pp. 552–557.
DOI: https://doi.org/10.1134/S1023193519060156

[32] Ponomarev I.I., Razorenov D.Y., Ponomarev I.I., et al. Synthesis and studies of polybenzimidazoles for high-temperature fuel cells. *Russ. J. Electrochem.,* 2014, vol. 50, no. 7, pp. 694–699. DOI: https://doi.org/10.1134/S1023193514070118

[33] Ponomarev I.I., Ponomarev I.I., Filatov I.Y., et al. Design of electrodes based on a carbon nanofiber nonwoven material for the membrane electrode assembly of a polybenzimidazole-membrane fuel cell. *Dokl. Phys. Chem.,* 2013, vol. 448, no. 2, pp. 23–27. DOI: https://doi.org/10.1134/S0012501613020036

[34] Ponomarev I.I., Skupov K.M., Zhigalina O.M., et al. New carbon nanofiber composite materials containing lanthanides and transition metals based on electrospun polyacrylonitrile for high temperature polymer electrolyte membrane fuel cell cathodes. *Polymers,* 2020, vol. 12, iss. 6, art. 1340. DOI: https://doi.org/10.3390/polym12061340

[35] Pomomarev I.I., Razorenov D.Yu., Ponomarev I.I., et al. Polybenzimidazoles *via* polyamidation: a more environmentally safe process to proton conducting membrane for hydrogen HT-PEM fuel cell. *Eur. Polym. J.*, 2021, vol. 156, art. 110613.
DOI: https://doi.org/10.1016/j.eurpolymj.2021.110613

[36] Skupov K.M., Ponomarev I.I., Volfkovich Y.M., et al. Porous structure optimization of electrospun carbon materials. *Russ. Chem. Bull.*, 2020, vol. 69, no. 6, pp. 1106–1113. DOI: https://doi.org/10.1007/s11172-020-2875-7

[37] Skupov K.M., Ponomarev I.I., Vol'fkovich Y.M., et al. The effect of the stabilization and carbonization temperatures on the properties of microporous carbon nanofiber cathodes for fuel cells on polybenzimidazole membrane. *Polym. Sci. Ser. C,* 2020, vol. 62, no. 2, pp. 231–237. DOI: https://doi.org/10.1134/S1811238220020149

[38] Dong Z., Kennedy S.J., Wu Y. Electrospinning materials for energy-related applications and devices. *J. Power Sources*, 2011, vol. 196, iss. 11, pp. 4886–4904.
DOI: https://doi.org/10.1016/j.jpowsour.2011.01.090

[39] Inagaki M., Yang Y., Kang F. Carbon nanofibers prepared via electrospinning. *Adv. Mater.*, 2012, vol. 24, iss. 19, pp. 2547–2566.
DOI: https://doi.org/10.1002/adma.201104940

[40] Tenchurin T.Kh., Krasheninnikov S.N., Orekhov A.S., et al. Rheological features of fiber spinning from polyacrylonitrile solutions in an electric field. Structure and properties. *Fibre Chem.*, 2014, vol. 46, no. 3, pp. 151–160.
DOI: https://doi.org/10.1007/s10692-014-9580-y

[41] Yusof N., Ismail A.F. Post spinning and pyrolysis processes of polyacrylonitrile (PAN)-based carbon fiber and activated carbon fiber: a review. *J. Anal. Appl. Pyrol.*, 2012, vol. 93, pp. 1–13. DOI: https://doi.org/10.1016/j.jaap.2011.10.001

[42] Zhang B., Kang F., Tarascon J.-M., et al. Recent advances in electrospun carbon nanofibers and their application in electrochemical energy storage. *Prog. Mater. Sci.*, 2016, vol. 76, pp. 319–380. DOI: https://doi.org/10.1016/j.pmatsci.2015.08.002

[43] Kopeć M., Lamson M., Yuan R., et al. Polyacrylonitrile-derived nanostructured carbon materials. *Prog. Polym. Sci.*, 2019, vol. 92, pp. 89–134.
DOI: https://doi.org/10.1016/j.progpolymsci.2019.02.003

[44] Rouquerol J., Rouquerol F., Sing K.S.W., et al. Adsorption by powders and porous solids: principles, methodology and applications. Academic Press, 2012.

[45] Linares-Solano A., Stoeckli F. Commentary on the paper "On the adsorption affinity coefficient of carbon dioxide in microporous carbons" by E.S. Bickford et al. (Carbon 2004; 42: 1867–71). *Carbon*, 2005, vol. 43, iss. 3, pp. 658–660.
DOI: https://doi.org/10.1016/j.carbon.2004.10.007

[46] Ewing M.B., Lilley T.H., Olofsson G.M., et al. Standard quantities in chemical thermodynamics. Fugacities, activities and equilibrium constants for pure and mixed phases (IUPAC Recommendations 1994). *Pure Appl. Chem.*, 1994, vol. 66, iss. 3, pp. 533–552. DOI: https://doi.org/10.1351/pac199466030533

Vtyurina Elizaveta S. — Master's Degree (Mater. Sc.), Junior Researcher, A.N. Nesmeyanov Institute of Organoelement Compounds of Russian Academy of Sciences (Vavilova ul. 28, str. 1, Moscow, 119334 Russian Federation).

Ponomarev Igor I. — Dr. Sc. (Chem.), Professor; Principal Researcher and Head of Laboratory, A.N. Nesmeyanov Institute of Organoelement Compounds of Russian Academy of Sciences (Vavilova ul. 28, str. 1, Moscow, 119334 Russian Federation).

Buyanovskaya Anastasia G. — Cand. Sc. (Chem.), Principal Researcher and Head of Laboratory, A.N. Nesmeyanov Institute of Organoelement Compounds of Russian Academy of Sciences (Vavilova ul. 28, str. 1, Moscow, 119334 Russian Federation).

Ponomarev Ivan I. — Cand. Sc. (Chem.), Senior Researcher, A.N. Nesmeyanov Institute of Organoelement Compounds of Russian Academy of Sciences (Vavilova ul. 28, str. 1, Moscow, 119334 Russian Federation).

Skupov Kirill M. — Ph.D. (Chem.), Senior Researcher, A.N. Nesmeyanov Institute of Organoelement Compounds of Russian Academy of Sciences (Vavilova ul. 28, str. 1, Moscow, 119334 Russian Federation).